The Journal of Nutrition
Biochemical, Molecular, and Genetic Mechanisms

Deletion of *Tis7* Protects Mice from High-Fat Diet-Induced Weight Gain and Blunts the Intestinal Adaptive Response Postresection[1–3]

Cong Yu,[4,9] Shujun Jiang,[4,9] Jianyun Lu,[4] Carrie C. Coughlin,[4] Yuan Wang,[4] Elzbieta A. Swietlicki,[4] Lihua Wang,[4] Ilja Vietor,[8] Lukas A. Huber,[8] Domagoj Cikes,[8] Trey Coleman,[5] Yan Xie,[4] Clay F. Semenkovich,[5] Nicholas O. Davidson,[4,6] Marc S. Levin,[4,7] and Deborah C. Rubin[4,6]*

Divisions of [4]Gastroenterology and [5]Endocrinology, Metabolism and Lipid Research, Department of Medicine, and [6]Department of Developmental Biology, Washington University School of Medicine, St. Louis, MO 63110; [7]Department of Medicine, St. Louis Veterans Administration Medical Center, St. Louis, MO 63106; and [8]Biocenter, Division of Cell Biology, Innsbruck Medical University, Innsbruck 6010, Austria

Abstract

After loss of intestinal surface area, the remaining bowel undergoes a morphometric and functional adaptive response. Enterocytic expression of the transcriptional coregulator tetradecanoyl phorbol acetate induced sequence 7 (*Tis7*) is markedly increased in a murine model of intestinal adaptation. Mice overexpressing *Tis7* in intestine have greater triglyceride absorption and weight gain when fed a high-fat diet (42% energy) than their wild-type (WT) littermates fed the same diet. These and other data suggest that Tis7 has a unique role in nutrient absorptive and metabolic adaptation. Herein, male $Tis7^{-/-}$ and WT mice were fed a high-fat diet (42% energy) for 8 wk. Weight was monitored and metabolic analyses and hepatic and intestinal lipid concentrations were compared after 8 wk. Intestinal lipid absorption and metabolism studies and intestinal resection surgeries were performed in separate groups of $Tis7^{-/-}$ and WT mice. At 8 wk, weight gain was less and jejunal mucosal and hepatic triglyceride and cholesterol concentrations were lower in $Tis7^{-/-}$ mice than in the WT controls. Following corn oil gavage, serum cholesterol, triglyceride, and FFA concentrations were lower in the $Tis7^{-/-}$ mice than in the WT mice. Incorporation of oral ^{3}[H] triolein into intestinal mucosal cholesterol ester and FFA was less in $Tis7^{-/-}$ compared with WT mice. Following resection, crypt cell proliferation rates and villus heights were lower in $Tis7^{-/-}$ than in WT mice, indicating a blunted adaptive response. Our results suggest a novel physiologic function for *Tis7* in the gut as a global regulator of lipid absorption and metabolism and epithelial cell proliferation. J. Nutr. 140: 1907–1914, 2010.

Introduction

Short bowel syndrome results from loss of functional small bowel surface area due to surgical resection for therapy of Crohn's disease or from trauma, ischemia, radiation enteritis, or other small bowel injuries. Following loss of small bowel, the remaining intestine undergoes an adaptive response characterized by increased crypt cell proliferation and enhanced villus height and crypt depth, resulting in increased functional absorptive capacity (1,2). The amount of residual normal small bowel and colon and the robustness of the adaptive response determine whether patients with short bowel syndrome can continue to eat normally or require parenteral nutrition for nutritional support. Elucidation of the mechanisms that regulate this response can lead to the design of novel therapeutic agents, as recently demonstrated in clinical trials utilizing an analogue of glucagon-like peptide 2 (GLP-2)[10] to enhance the gut adaptive response (3,4).

We have previously shown that in rodent models of short bowel syndrome, expression of the transcriptional coregulator Tis7 is markedly increased in the rodent adaptive small bowel post resection (5,6) and its expression in epithelial cells is regulated by a GLP-2 analogue (6). To further explore the role of Tis7 in the gut adaptive response, we previously generated

[1] Supported by NIH grants DK46122, DK61216, DK50466 (D.C.R.,M.S.L.), HL-38180, and DK-56260 (N.O.D.); by the Morphology and Functional Genomics Cores of The Washington University Digestive Diseases Research Core Center P30 DK52574; by the Clinical Nutrition Research Unit DK56341, and by Austrian Science Fund (FWF) grant P18531 (I.V.).

[2] Author disclosures: C. Yu, S. Jiang, J. Lu, C. C. Coughlin, Y. Wang, E. A. Swietlicki, L. Wang, I. Vietor, L. A. Huber, D. Cikes, T. Coleman, Y. Xie, C. F. Semenkovich, N. O. Davidson, M. S. Levin, and D. C. Rubin, no conflicts of interest.

[3] Supplemental Tables 1–4 are available with the online posting of this paper at jn.nutrition.org.

[9] Contributed as first authors.

* To whom correspondence should be addressed. E-mail: drubin@wustl.edu.

[10] Abbreviations used: RER, respiratory exchange ratio; q, quantitative real-time; $Tis7^{tg}$, *Tis7* transgenic; WUSM, Washington University School of Medicine; WT, wild type.

Manuscript received June 29, 2010. Initial review completed July 01, 2010. Revision accepted August 26, 2010.
First published online September 22, 2010; doi:10.3945/jn.110.127084.

transgenic mice that overexpress Tis7 (*Tis7*^{tg}) in the small bowel and proximal colon (7). These mice had shorter villi in the proximal small intestine and reduced small bowel length. Nevertheless, when subjected to partial small bowel resection, *Tis7*^{tg} mice exhibited a normal adaptive response. Pro-daptive changes in lipid trafficking were also observed. When fed a low-fat, nonpurified (control) diet, intestinal *Tis7*^{tg} mice weighed less than their wild-type (WT) littermates and had less body surface area but had greater whole body adipose tissue mass. Intestinal *Tis7*^{tg} mice also exhibited accelerated weight gain and an additional increase in adiposity when fed a high-fat (42% energy) diet compared with WT mice (7,8). This phenotype was associated with fat accumulation in the liver and the small bowel and an increase in the rate of triglyceride absorption from the lumen into serum, as documented by a rapid rise in serum triglyceride and FFA concentrations after oral lipid challenge. The expression of several candidate genes associated with enterocytic triglyceride absorption, including diacylglycerol acyltransferase (*Dgat*) 1, *Dgat2*, and microsomal triglyceride transfer protein (*Mttp*), was greater in intestinal *Tis7*^{tg} mice receiving both low-fat, nonpurified (control) and high-fat (42% energy) diets. Thus, we postulated that Tis7 may play a unique role in the gut adaptive response, enhancing intestinal triglyceride absorption and increasing adiposity, both of which are clearly advantageous for mammals with nutritional compromise due to short bowel syndrome.

To further elucidate the role of Tis7 in the gut adaptive response, we now report our findings in *Tis7*$^{-/-}$ mice, generated as described in (8). Our data suggest that Tis7 plays an important role in both the functional and morphometric adaptive responses following loss of small bowel surface area.

Materials and Methods

Mice

All animal experimentation was approved by the Animal Studies Committee of the Washington University School of Medicine (WUSM). WT or *Tis7*$^{-/-}$ (on a C57Bl/6 background) mice were generated as per (8). Mice were housed in WUSM animal facilities and maintained on a strict 12-h:12-h light/dark cycle with ad libitum consumption of the control diet (Picolab 20, Ralston Purina), containing 200 g protein, 99 g fat, 47 g fiber, and an energy value of 14.24 MJ/kg diet (9), and water. The experimental diets for fat feeding and intestinal resection experiments are described below.

Tissue preparation for histochemical and immunohistochemical analyses

Mice were killed using isoflurane anesthetic. The intestine, liver, heart, and skeletal muscle were rapidly removed. The intestine was rinsed and then suspended with a fixed weight to measure the length. A duodenal segment was obtained and the remaining intestine was divided into a proximal jejunal (proximal third of remaining intestine), distal jejunal (middle third), and ileal (distal third) segments. The harvested segments were different for the intestinal resection experiments (see below). Tissues were frozen in liquid nitrogen for RNA and protein isolation and placed in optimal cutting temperature solution or in formalin for histochemical and immunohistochemical analysis. Histologic studies were performed in the Morphology Core of the WUSM Digestive Diseases Research Core Center. For morphometric analyses, paraffin-embedded tissues were stained with hematoxylin and eosin. Fat droplets were analyzed using frozen sections stained with Oil Red O as described (7). Formalin-fixed, paraffin-embedded tissues were used for immunohistochemical detection of 5-bromodeoxyuridine incorporation into DNA using a monoclonal anti-bromodeoxyuridine antibody (Zymed Laboratories) and streptavidin-biotin amplification (10).

Expt. 1: High-fat diet

Weight- and age-matched (7–10 wk old) male *Tis7*$^{-/-}$ mice and WT controls were fed a synthetic, high-saturated fat (Western) diet for 8 wk [Adjusted Calories Diet TD 88137, Harlan Teklad, containing 173 g protein, 210 g milk fat, and 1.5 g cholesterol/kg diet with 42% of total energy from fat and an energy value of 18.84 MJ/kg diet (9)] (**Supplemental Table 1**). Mice were weighed every 2–3 d after beginning the high-fat diet (n = 5/group).

Quantitation of food consumption and fecal fat. At the beginning of wk 5, the mice were transferred to metabolic cages containing inserts that permitted collection of wasted food and prevented coprophagia. The quantity of food ingested per mouse was measured every 2–3 d for 7–11 d. Feces were collected every 2–3 d for 1 wk and fecal fat was quantitated following extraction with 2:1 chloroform:methanol (11).

Body composition analysis. During wk 8 of the high-fat diet, body composition analyses of awake mice were performed with MRI following the manufacturer's protocol (EchoMRI 3–1, Echo Medical Systems). The device included a permanent magnet with a transmitter/antenna that allowed for acquisition of unobscured signals from all elements of a 3-dimensional body and permitted the direct evaluation of fat and lean tissue and free liquids. Anesthesia was not required and each analysis required ~2 min.

Basal metabolic rate measurements and mouse activity measurements. During wk 8, oxygen consumption and carbon dioxide production were studied at room temperature using single chamber indirect calorimetry to measure (Oxymax System, Columbus Instruments) as per (12,13). To measure physical activity, infrared sensors were utilized to detect body heat and its spatial displacement over time [InfraMot Activity System, TSE Systems as per (14) and the manufacturer's brochure]. Sensors were mounted on mouse cage covers and data analyzed by InfraMot software (v. 1.3), which provided a relative measure of duration and intensity of the activity (time moving/total time).

Tissue analyses. At the end of 8 wk of the high-fat diet the mice were killed. Heart, liver, skeletal muscle, and small intestinal segments were harvested for Oil Red O staining to detect lipid accumulation. Liver and intestinal samples were collected for RNA isolation and for quantification of total triglycerides, cholesterol, FFA, and phospholipids. For lipid analysis, tissues were frozen, extracted with chloroform/methanol, and assayed enzymatically using the L-type triglyceride H kit, the cholesterol E kit, the NEFA-HR(2) microtiter procedure kit, and the phospholipid B-kit, respectively (Wako Diagnostics, Wako Chemicals USA) (15). Data were normalized to tissue weight.

Microarray and quantitative real-time RT-PCR analysis of intestinal gene expression. Total RNA was prepared using TRIzol Reagent (Invitrogen) according to the manufacturer's protocol. RNA quality was assessed using an Agilent 2100 Bioanalyzer. RNA was labeled using the Agilent low RNA input linear amplification kit. The resulting probes were hybridized to Agilent DNA microarrays containing 41,000+ mouse genes and transcripts (Agilent). Probe preparations and hybridizations were performed in the WUSM Genomics Core of the Digestive Diseases Research Core. Data are reported as the ratio of means comparing *Tis7*$^{-/-}$ to WT. Changes in gene expression identified by microarray analysis were verified for selected genes using quantitative real-time (q) RT-PCR. qRT-PCR was also used to analyze the expression of genes with roles in intestinal lipid absorption and genes that are members of the Hedgehog (Hh), Wingless-type MMTV integration site (Wnt), and bone morphogenetic protein (Bmp) gene families. Database identifier numbers are from the National Center for Biotechnology Information (16). For qRT-PCR, jejunal RNA was treated with DNase I using the DNA-free kit (Ambion). First- strand cDNA was synthesized from 1 μg RNA using Super-Script II RT (Invitrogen) with random hexamer primers. qRT-PCR was performed on an SDS 7000 (Applied Biosystems) machine using 2× Sybr Green Master mix (Applied Biosystems). Oligonucleotide primers (**Supplemental Table 2**) (17) were chosen using Primer Express software

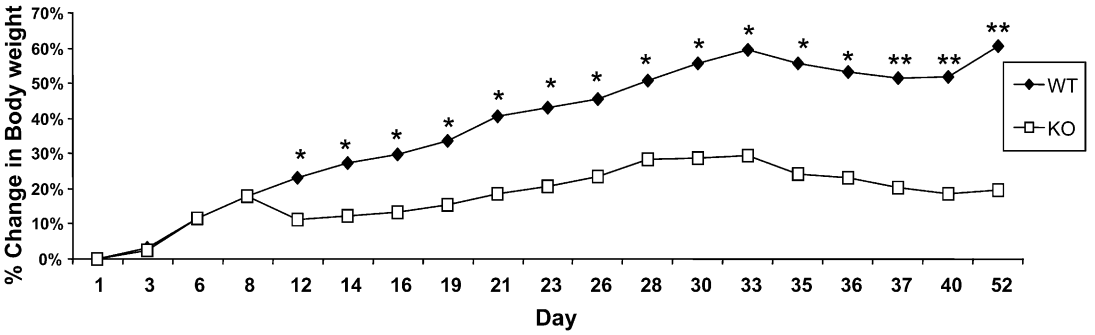

FIGURE 1 Growth curves of *Tis7*$^{-/-}$ [knockout (KO)] and WT male mice fed a high-fat diet for 8 wk (Expt. 1). Values are means, $n = 5$. Asterisks indicate different from KO: $*P < 0.05$; $**P = 0.001$.

(Applied Biosystems). For all primer sets, the kinetics of the RT-PCR was confirmed by serial dilutions of different cDNA preparations. Amplification of 18s ribosomal RNA was used for normalization and quantification was done by the comparative Ct method (user bulletin no. 2, Applied Biosystems).

Expt. 2: Analysis of in vivo intestinal triglyceride (corn oil) absorption

Triglyceride absorption experiments were performed as previously described (7) with the following modifications: *Tis7*$^{-/-}$ mice and WT littermates maintained on the control diet were feed deprived for 4 h. Serum was obtained from feed-deprived mice for measurement of triglyceride, cholesterol, and FFA concentrations. Mice were then i.v. injected with 1 g/kg of pluronic F127 (Invitrogen) to inhibit lipolysis and clearance of triglyceride-rich lipoproteins (18). At 15 min after the injection, mice were gavaged with 500 μL of corn oil. Groups of mice ($n = 5$) were killed 4 and 24 h later. Serum triglycerides, FFA, cholesterol, and glucose concentrations were measured at t = 0, 4, and 24 h utilizing core facilities of the WUSM Clinical Nutrition Research Unit. Tissues were harvested as above for histochemical analysis by hematoxylin and eosin and Oil Red O staining.

Expt. 3: Analysis of in vivo ^{3}H-triolein absorption

Tis7$^{-/-}$ or WT mice fed the control diet were feed deprived overnight and serum was obtained for measurement of triglyceride, cholesterol, and FFA concentrations. Mice were injected with pluronic F127 as described in Expt. 2. After 30 min, mice were gavaged with a tracer of (9,10) ^{3}H-triolein (10 μL, 37 kBq/μL, American Radiochemical) mixed with corn oil (90 μL) and Intralipid (400 μL; Baxter). At 2 h postgavage, serum was collected. At 4 h, mice were killed and serum and small intestine were collected for lipid analysis and quantitation of ^{3}H-labeled fatty acids as per (19). The small intestine was divided into thirds, opened, and rinsed. The luminal contents were saved and the mucosa was then scraped and frozen in liquid nitrogen.

Expt. 4: Analysis of intestinal adaptation

Male 3-mo-old *Tis7*$^{-/-}$ or WT mice were fed an AIN93M liquid diet (Dyets Liquid Diet no. 10080, containing 38.7 g protein, 11.0 g fat/L diet with an energy value of 16.74 MJ/L diet) (**Supplemental Table 3**). Individually caged mice consumed ad libitum the diet for 1 wk prior to surgery. A liquid diet was used to reduce the incidence of intestinal obstruction following resection surgery (17,20). Mice were anesthetized with ketamine HCl (87 mg/kg)/xylazine HCl (13 mg/kg) and underwent 50% bowel resection. The resection was begun 2–3 cm distal to the ligament of Treitz and extended to 8 cm proximal to the ileocecal valve as described previously (6,7,17,20). The distal ileum of the resected intestine was fixed in formalin for morphometric analysis. An end-to-end anastomosis was formed between the remnant jejunum and ileum using 9–0 silk sutures. All mice received gentamicin as a prophylactic antibiotic (0.2 mg in 0.5 mL of saline intraperitoneally) and buprenorphine (0.03 mg/kg subcutaneously) for analgesia. Mice were killed with inhalational isoflurane 72 h after surgery. The remnant intestine was divided into duodenal-jejunal and ileal segments that were fixed in formalin, frozen in optimal cutting temperature solution, or placed into liquid nitrogen. qRT-PCR (as described above) was used to compare the expression of members of the Bmp, Wnt, and Hh gene families in the remnant ileum of *Tis7*$^{-/-}$ and WT resected mice.

Intestinal morphometric analyses. Villus heights, crypt depths, and crypt cell numbers were measured in the resected ileum and the remnant intestine in at least 7–10 well-oriented, full-length crypt-villus units as per (7,17,20). Crypt cell proliferation was measured by 5-bromodeoxyuridine incorporation into DNA (17) and reported as the percentage of labeled cells per full-length crypt (i.e. number of labeled cells divided by the total number of cells per crypt).

Statistical analyses

For most experiments, means were calculated and compared between WT and *Tis7*$^{-/-}$ mice using a Student's *t* test. For comparison of villus heights and crypt depths in WT and *Tis7*$^{-/-}$ mice pre- and postsurgery, 2-way repeated ANOVA was performed with Tukey's post hoc test (Sigma Stat). Values in the text are means ± SEM. Differences were considered significant at $P \leq 0.05$.

Results

Tis7$^{-/-}$ *mice are protected from high-fat diet-induced weight gain.* The effects of *Tis7* deletion on high-fat diet-induced weight gain were examined in Expt. 1. In contrast to WT mice, *Tis7*$^{-/-}$ mice gained less weight when fed the high fat-diet (**Fig. 1**). The change in weight gain in *Tis7*$^{-/-}$ mice was evident by as early as 12 d and persisted for up to 8 wk.

This protection from weight gain was not due to differences in food consumption or in the overall quantity of lipid absorbed, because fecal fat (data not shown) as well as fecal weight were the same in *Tis7*$^{-/-}$ and WT mice (**Supplemental Table 4**). *Tis7*$^{-/-}$ and WT mice also did not differ in physical activity rates

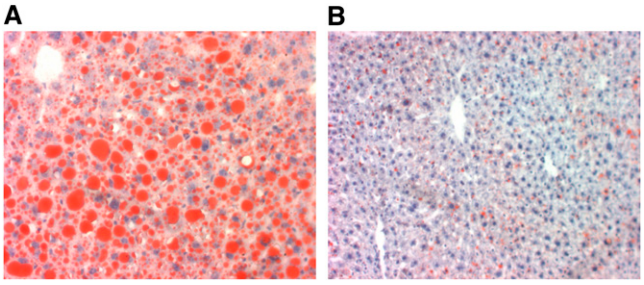

FIGURE 2 Hepatic lipid accumulation in WT (*A*) *Tis7*$^{-/-}$ (*B*) mice fed a high-fat diet for 8 wk (Expt. 1). Sections were stained with Oil Red O to detect lipid. In *A*, note the large red fat globules in hepatocytes. Fat accumulation is markedly less in *B*.

TABLE 1 Hepatic and intestinal lipid concentrations in WT and *Tis7*$^{-/-}$ mice fed a high-fat diet for 8 wk (Expt. 1)[1]

	Cholesterol, *μmol/g*		Triglycerides, *μmol/g*		FFA, *nmol/g*		Phospholipids, *μmol/g*	
	WT	*Tis7*$^{-/-}$	WT	*Tis7*$^{-/-}$	WT	*Tis7*$^{-/-}$	WT	*Tis7*$^{-/-}$
Liver	2.58 ± 0.59	0.75 ± 0.31*	8.24 ± 0.44	2.03 ± 0.50*	2.10 ± 0.17	1.07 ± 0.13*	4.14 ± 0.33	4.00 ± 0.28
Proximal intestine	1.22 ± 0.10	0.84 ± 0.08*	40.79 ± 8.46	19.15 ± 4.60*	21.73 ± 6.53	12.14 ± 3.29	3.07 ± 0.26	2.65 ± 0.13
Distal intestine	1.81 ± 0.17	1.79 ± 0.29	790.10 ± 84.20	930.59 ± 200.74	44.99 ± 7.02	92.18 ± 16.71*	1.76 ± 0.15	1.88 ± 0.32

[1] Values are means ± SEM. For liver lipids, $n = 5$ (*Tis7*$^{-/-}$ and WT); for proximal intestine, $n = 5$ (*Tis7*$^{-/-}$) or 4 (WT); for distal intestine, $n = 5$ (*Tis7*$^{-/-}$ and WT) except triglycerides, $n = 4$ (*Tis7*$^{-/-}$ and WT). *Different from WT, $P < 0.05$.

and basal metabolic rates as measured by indirect calorimetry (Supplemental Table 4).

Protection from adiposity in high fat-fed Tis7$^{-/-}$ *mice (Expt. 1).* The differences in weight gain between the *Tis7*$^{-/-}$ and WT mice were reflected by differences in total body fat mass. Total adiposity, expressed as grams of body fat, was markedly less in the *Tis7*$^{-/-}$ compared with WT mice at 8 wk ($P < 0.0001$), whereas lean body mass was unchanged in *Tis7*$^{-/-}$ compared with WT mice (Supplemental Table 4).

Previous studies showed that intestinal *Tis7*^{tg} mice rapidly developed fatty livers after 2 wk of high-fat (42% energy) feeding (7). To determine whether *Tis7*$^{-/-}$ mice were protected from diet-induced fatty liver, Oil Red O staining was performed on livers harvested from WT and *Tis7*$^{-/-}$ mice from Expt. 1 (**Fig. 2***A*,*B*). WT mice (Fig. 2*A*) had a marked accumulation of fat, whereas *Tis7*$^{-/-}$ livers were relatively spared (Fig. 2*B*) Consistent with the Oil Red O staining patterns, hepatic triglyceride, FFA, and cholesterol concentrations were lower in *Tis7*$^{-/-}$ compared with WT mice (**Table 1**). The phospholipid concentration was unchanged in *Tis7*$^{-/-}$ compared with WT mice. WT and *Tis7*$^{-/-}$ mice did not differ in Oil Red O staining of heart or skeletal muscle.

Triglyceride, cholesterol, and FFA absorption are altered in Tis7$^{-/-}$ *mice.* Based on our previous findings in *Tis7*^{tg} mice (7), which showed an increase in the rate of intestinal triglyceride absorption, we hypothesized that *Tis7* deletion might result in delayed triglyceride and FFA absorption. Proximal intestinal triglyceride and cholesterol concentrations were lower in high fat-fed *Tis7*$^{-/-}$ compared with WT mice from Expt. 1 (Table 1). FFA and phospholipid concentrations were unchanged.

The proximal small intestinal lipid content was lower in *Tis7*$^{-/-}$ mice compared with WT controls, yet fecal fat was not greater in *Tis7*$^{-/-}$ mice, suggesting that unabsorbed fats may be shunted to and absorbed by the distal bowel. Consistent with this suggestion, FFA concentrations in the distal small bowel were significantly higher in *Tis7*$^{-/-}$ compared with WT mice (from Expt. 1) (Table 1). However, phospholipid, cholesterol, and triglyceride concentrations were unchanged. Thus, *Tis7* deletion decreases lipid absorption most prominently in the proximal small bowel, with shunting of FFA to distal gut.

To examine more closely the dynamic alterations in intestinal lipid uptake, *Tis7*$^{-/-}$ and WT mice received a corn oil bolus ([Expt. 2; as per (18)]. At 4 h after the corn oil bolus gavage, serum triglyceride, FFA, and cholesterol concentrations were significantly lower in *Tis7*$^{-/-}$ compared with WT mice (**Table 2**). At 24 h after the gavage, there were no longer significant differences in serum cholesterol, FFA, and triglyceride concentrations between *Tis7*$^{-/-}$ and WT mice. Serum glucose concentrations were unchanged in *Tis7*$^{-/-}$ compared to WT mice following food deprivation for 4 h, or after corn oil bolus.

To further define the differences in lipid absorption and metabolism from proximal to distal intestine, mice were gavaged with ^{3}H triolein mixed with Intralipid and corn oil (Expt. 3). Serum triglyceride concentrations were lower in *Tis7*$^{-/-}$ compared with WT mice at 2 h after lipid gavage ($P < 0.05$). Recovered radiolabel in serum at 4 h following gavage did not significantly differ between the 2 groups. However, the distribution of ^{3}H triolein among different lipid classes was altered in the *Tis7*$^{-/-}$ mice compared with WT mice in the proximal, middle, and distal small intestines (**Fig. 3**). The relative abundance of cholesterol esters was significantly lower in *Tis7*$^{-/-}$ compared with WT mice in the proximal mid (Fig. 3*A*) and distal (Fig. 3*B*) intestines (data not shown). The relative abundance of FFA was significantly lower in the mid (Fig. 3*A*) and distal (Fig. 3*B*) intestine of *Tis7*$^{-/-}$ compared with WT mice. In contrast, the relative abundance of triglycerides was significantly higher in the distal gut.

Expression of genes involved in enterocytic fatty acid uptake and processing in Tis7$^{-/-}$ *jejunum after chronic high-fat feeding.* Compared with WT mice, intestinal *Tis7*^{tg} (transgenic) mice express greater levels of the lipid trafficking proteins *Dgat 1*, *Dgat 2*, and *Mttp*. To further assess the role of Tis7 in intestinal lipid metabolism, expression of these and other genes involved in adipogenesis and triglyceride processing was studied with microarray analyses and qRT-PCR (**Table 3**) using mRNA isolated from jejunum of WT and *Tis7*$^{-/-}$ mice from Expt. 1. *Insulin-like growth factor binding protein 1* (*Igfbp1*) mRNA, which encodes a binding protein that regulates insulin-like growth factor 1 levels and affects adipogenesis, was markedly lower in the gut of high fat-fed *Tis7*$^{-/-}$ mice ($P = 0.04$). Expression of *Dgat1* ($P = 0.08$) tended to be lower. Expression of *Dgat2*; *cluster of differentiation 36* (*Cd36*), a putative intestinal fatty acid transporter; the *Niemann-Pick C1-like 1 protein* (*Npc1L1*), a cholesterol transporter; *cytochrome p450 4a14* (*cyp4a14*); *ATP-binding cassette sub-family G member 5* (*Abcg5*); *Lipin 1*; and *Mttp* did not differ between the groups ($P > 0.1$).

TABLE 2 Serum triglyceride, cholesterol, FFA, and glucose concentrations in WT or *Tis7*$^{-/-}$ mice at 4 h following an i.g. corn oil bolus (Expt. 2)[1]

	WT	*Tis7*$^{-/-}$
Triglycerides, *mmol/L*	25.9 ± 1.50	17.8 ± 2.76*
Cholesterol, *mmol/L*	3.66 ± 0.20	2.79 ± 0.21*
FFA, *mmol/L*	6.80 ± 0.59	4.30 ± 0.54*
Glucose, *mmol/L*	15.1 ± 0.81	13.5 ± 0.66

[1] Values are means ± SEM, $n = 6$ (*Tis7*$^{-/-}$) or 7 (WT). *Different from WT, $P < 0.05$.

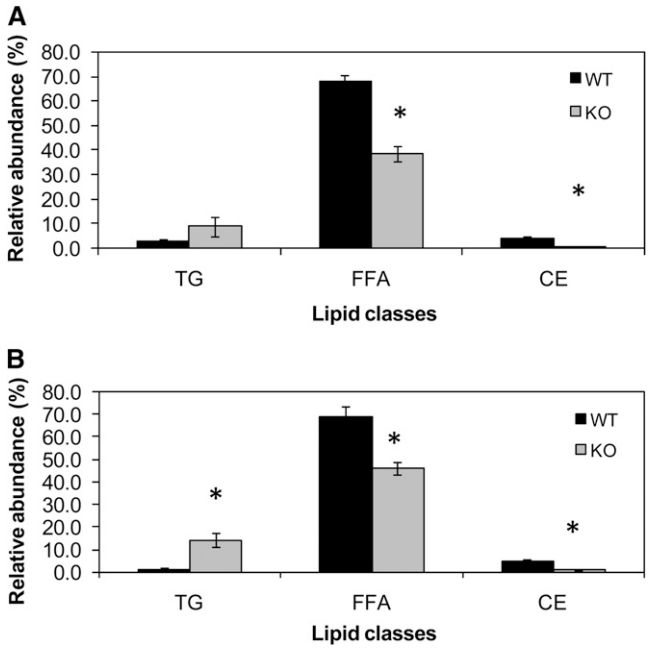

FIGURE 3 Relative abundance of triglycerides, FFA, and cholesterol esters in the jejunal (*A*) and ileal (*B*) mucosa of *Tis7*$^{-/-}$ and WT mice at 4 h after receiving an i.g. bolus of ^{3}H triolein (Expt. 3). Bars represent means ± SEM, $n = 7$. *Different from WT, $P < 0.05$.

Deletion of Tis7 results in inhibition of morphometric small bowel adaptation and diminished Hh and Wnt signaling activity. To examine the functional consequences of *Tis7* deletion, 3-mo-old *Tis7*$^{-/-}$ and WT mice were subjected to 50% small bowel resection (Expt. 4). *Tis7*$^{-/-}$ mice exhibited a blunted adaptive response. Crypt cell proliferation rates were significantly lower in *Tis7*$^{-/-}$ compared with WT mice following resection (**Table 4**). Furthermore, in WT but not *Tis7*$^{-/-}$ mice, villus heights were greater compared with preoperative controls in the remnant intestine at 72 h post resection (**Table 5**). After resection, villus heights in the remnant intestine of *Tis7*$^{-/-}$ mice were significantly lower than in WT mice. Crypt depths were greater in WT and *Tis7*$^{-/-}$ mice following resection compared with the respective preoperative controls. By 10 d after surgery, the differences in proliferation and villus height resolved (data not shown).

TABLE 3 Expression of genes that regulate intestinal lipid metabolism in jejunum of high fat-fed *Tis7*$^{-/-}$ mice (Expt. 1)[1]

Gene[2]	% of WT
Cd36 (12491)	67
Igfbp1 (16006)	33*
Cyp4A14 (13119)	56
Dgat1 (13350)	54
Dgat2 (67800)	60
Npc1L1 (237636)	65
Mttp (17777)	99
C/ebpβ (12608)	135
Abcg5 (27409)	78
Lpin1 (14245)	79

[1] Values are percentages, $n = 3$ (*Tis7*$^{-/-}$ and WT). *Different from WT, $P = 0.04$.
[2] Database gene identifier numbers from (16).

In vitro studies in cultured cells have shown that *Tis7* is a transcriptional coregulator that functions by interacting with the mSin3B complex and histone deacetylases and may act to inhibit or increase transcription of selected target genes (21–23). Expression of Hh signaling pathway members, including *Gli1* and *Gli2*, transcriptional targets of Hh that are markers of Hh signaling activity, and *Hedgehog interacting protein* (*Hhip*), which also reflects Hh signaling, were significantly lower in *Tis7*$^{-/-}$ compared with WT remnant ileum (Expt. 4) (**Table 6**). *Gli3* trended to be lower ($P = 0.09$) and there were no significant changes in Hh ligand [*Indian Hedgehog* (*Ihh*), *Desert hedgehog* (*Dhh*)], *Patched 1* (*Ptc1*) or *Patched 2* (*Ptc2*)] receptor expression. In addition, several downstream targets of Wnt signaling, including *Ephrin B2* and *Cyclin D1*, were also lower, whereas *Bmp2* and *Bmp4* did not differ between the groups ($P > 0.1$).

Discussion

The central findings from this study are that *Tis7*$^{-/-}$ mice are protected from weight gain induced by the ingestion of a high-fat diet and *Tis7*$^{-/-}$ mice have a blunted early adaptive response. The former phenotype was associated with decreased whole body adiposity but no change in food consumption, fecal fat content, or activity in *Tis7*$^{-/-}$ mice compared with WT controls. Several observations suggest that changes in intestinal lipid trafficking as well as hepatic lipid metabolism may account for the observed reduced adiposity. Compared with WT mice, *Tis7*$^{-/-}$ mice chronically fed a high-fat diet had lower proximal intestinal triglyceride and cholesterol levels and markedly lower hepatic cholesterol, triglyceride, and FFA levels as well. In mice fed the high-fat diet, ileal FFA levels were greater in *Tis7*$^{-/-}$ mice compared with WT mice. Also consistent with a role for Tis7 in hepatic and intestinal lipid metabolism was the finding that serum triglyceride, cholesterol, and FFA concentrations were lower in *Tis7*$^{-/-}$ compared with WT mice at 4 h following gavage with corn oil. Following gavage with ^{3}H-triolein in corn oil and Intralipid, *Tis7*$^{-/-}$ compared with WT mice had lower mucosal concentrations of cholesterol esters (proximal and distal small bowel) and FFA (mid and distal jejunum and ileum) and greater concentrations of ileal triglycerides. These results suggest that *Tis7* deletion alters intestinal lipid metabolism, results in a decreased rate of intestinal triglyceride absorption, and may indicate a novel link between lipid absorption and the morphometric adaptive response. In agreement with our data from *Tis7*^{tg} mice (7), these results support the conclusion that *Tis7* is a mediator of intestinal lipid absorption and metabolism and plays a role in functional adaptation following gut resection.

The finding in *Tis7*$^{-/-}$ mice that changes in the rate of triglyceride absorption correlate to changes in body weight is consistent with data from other animal models. For example,

TABLE 4 Crypt cell proliferation indices in WT and *Tis7*$^{-/-}$ adaptive ileum at 72 h after 50% intestinal resection (Expt. 4)[1]

	Total crypt cells, *n*	Bromodeoxyuridine+ cells/crypt, *n*	Labeling index
WT	353 ± 68	94 ± 29	0.28 ± 0.04
Tis7$^{-/-}$	236 ± 35	25 ± 3*	0.11 ± 0.01*

[1] Values are means ± SEM, $n = 7$ (*Tis7*$^{-/-}$) or 8 (WT). *Different from WT, $P < 0.05$.

TABLE 5 Villus heights and crypt depths in *Tis7*$^{-/-}$ and WT ileum before surgery and at 72 h after 50% intestinal resection (Expt. 4)[1]

	Villus height μm		Crypt depth, μm	
	Presurgery	Postsurgery	Presurgery	Postsurgery
WT	265 ± 17.4[b]	421 ± 34.9[a]	92.5 ± 3.92[b]	115 ± 10.3[a]
Tis7$^{-/-}$	288 ± 21.9[b]	354 ± 32.1[b]	89.1 ± 4.21[b]	103 ± 7.03[a]

[1] Values are means ± SEM, n = 8 (*Tis7*$^{-/-}$) or 6 (WT). For each variable, labeled means without a common letter differ, $P < 0.05$. There was a significant effect of surgery and genotype on villus height and of surgery on crypt depth, but no effect of genotype.

TABLE 6 qRT-PCR analysis of expression of selected genes that regulate epithelial crypt cell proliferation in *Tis7*$^{-/-}$ vs. WT proximal ileum at 72 h post resection[1] (Expt.4)

Gene[2]	% of WT
Gli1 (14632)	27*
Hhip (15245)	36*
Gli2 (14633)	51*
Gli3 (14634)	50
EphB2 (13642)	66*
Cyclin D1 (12443)	51*
Ihh (16147)	61
Dhh (13363)	91
Ptc1 (19206)	63
Ptc2 (19207)	72
Bmp2 (12156)	124
Bmp4 (12159)	98

[1] Values are percentages, n = 5 (*Tis7*$^{-/-}$) or 4 (WT). Asterisks indicate different from WT: *$P \leq 0.05$.
[2] Database gene identifier numbers from (16).

intestinal alkaline phosphatase null mice exhibit increased weight gain when fed a high-fat diet, associated with an accelerated rate of lipid absorption (24). *Tis7*^{tg} mice show enhanced and rapid weight gain compared with WT controls, associated with an increased rate of lipid absorption (7). In contrast, *L-Fabp*$^{-/-}$ mice have slower intestinal lipid secretion kinetics and are protected against Western diet-induced obesity (19). These mice exhibited no difference in food consumption or fat absorption but did have reduced rates of appearance of triglyceride in the serum after a fat bolus. *Cd36*$^{-/-}$ mice are similarly protected from diet-induced obesity, possibly related to decreased formation and secretion of chylomicrons (26,27). *Cd36*$^{-/-}$ mice fed a high-fat diet have increased enterocytic lipid, defective triacylglycerol secretion by enterocytes, and slow clearance of lipoproteins derived from intestine. *Dgat1*-deficient mice have reduced postabsorptive chylomicronemia after a fat bolus and retain fat in enterocytes while fed a high-fat diet (28). These mice do not exhibit fat malabsorption but are lean and also are resistant to diet-induced obesity (29).

In chronically high fat-fed *Tis7*$^{-/-}$ mice, the concentration of ileal FFA was greater than in WT controls. In addition, when gavaged with radiolabeled triolein, the relative abundance of ileal triglycerides was greater in *Tis7*$^{-/-}$ mice compared with controls. These data suggest a shift in lipid absorption from the proximal to distal small intestine, which may also contribute to the decreased rate of absorption in *Tis7*$^{-/-}$ compared with WT mice.

The absorption of nutrients in addition to lipids may be directly or indirectly altered in *Tis7*$^{-/-}$ mice. Although beyond the scope of the current studies, indirect data suggest that carbohydrate absorption was unaltered in *Tis7*$^{-/-}$ mice. For example, serum glucose concentrations were unchanged in feed-deprived mice or after a lipid bolus (Table 2). Also, mRNA levels of the major glucose transporter SGLT1 were unchanged in our microarray analyses (data not shown).

When transfected into epithelial cells, *Tis7* functions as a transcriptional coregulator (22). Tis7 associates with the SIN3 complex to repress transcription by interacting with DNA binding proteins. Other data suggest that specific genes may also be induced, because the effects of Tis7 are cell-specific and Tis7 also acts to corepress inhibitors of transcriptional activity (23,30). Specific targets for Tis7-mediated repression include osteopontin and cellular retinoic acid binding protein II (22,31,32). The human homolog IFRD1 has been shown to act as a modifier gene for cystic fibrosis lung disease and regulates nuclear factor-κB p65 transactivation in mice (30). Our results suggest that *Tis7* has pleiotropic effects in intestinal epithelia. In *Tis7*^{tg} mice, genes involved in lipid transport such as *Dgat1*, *Dgat2*, *and Mttp* were upregulated (7). Deletion of *Tis7* resulted in a tendency toward lower jejunal expression of *Dgat1* (P = 0.08) but not *Dgat2*, *Npc1L1*, or *Cd36*. Full thickness jejunal samples were used for RNA extraction, thus reducing the sensitivity for detecting changes specific to the mucosa where these genes are preferentially expressed. *Tis7* deletion resulted in lower *Igfbp1* mRNA levels, which would be expected to raise effective IGF-1 concentrations. Because IGF-1 regulates gut proliferation and has effects on adipogenesis, this may represent an adaptive response to the decrease in adiposity and proliferation in the *Tis7*$^{-/-}$ mice.

In addition to decreased weight gain and diminished intestinal triglyceride absorption, *Tis7*$^{-/-}$ mice also exhibited lower crypt cell proliferation rates and villus lengths following small bowel resection. The early adaptive response is characterized by an increase in crypt cell proliferation over time and a presumptive expansion of the stem cell population (33), and *Tis7* expression is upregulated in the gut by 48 h after resection (*5*). The marked reduction in crypt cell proliferation rates resulting from *Tis7* deletion was associated with lower Hedgehog and Wnt signaling activity (Table 6). Wnt signaling plays a critical role in regulating gut epithelial proliferation (34), and Hh signaling is most active in the upper crypt and is required for normal gut epithelial cell differentiation (35). Thus, the observed reductions in crypt cell proliferation and villus heights are consistent with the changes in Wnt and Hh signaling. Our data also suggest a novel connection between enterocytic lipid accumulation and the regulation of crypt cell proliferation, possibly mediated via Hh and Wnt pathways. Other mouse models suggest these 2 observations may be linked. For example, the *Mttp-Iko* null mouse exhibits an increase in lipid accumulation and crypt cell proliferation rates (36). Neonatal mice treated with a Hh blocking antibody retain enterocytic lipid, associated with greater crypt cell proliferation (37). In addition, oral administration of SCFA or precursor fiber and resistant starches enhances the small bowel adaptive response and results in greater crypt cell proliferation (2). Little is known about the underlying mechanisms; however, fat feeding enhances GLP-2 release, a potent trophic enteroendocrine cell product. It is tempting to speculate that enhanced GLP-2 secretion in the *Mttp-Iko* null mouse or decreased secretion in the *Tis*$^{7-/-}$ mouse might be implicated in the regulation of the crypt cell proliferative response.

In summary, our results indicate a novel physiologic function for *Tis7* in the gut as a global regulator of lipid absorption and metabolism as well as epithelial cell proliferation. The precise mechanisms by which it acts in the whole animal have yet to be elucidated but are likely to include changes in gene expression that are either a direct result of *Tis7* deletion or reflect regulation of downstream targets. Further identification of these mechanisms may help identify novel therapeutic targets to enhance functional and morphometric adaptation following loss of functional small bowel surface area.

Acknowledgments

D.C.R., M.S.L., N.O.D., and C.F.S. designed research (project conception, development of overall research plan, and study oversight); C.Y., S.J., J.L., C.C.C., Y.W., E.A.S., L.W., T.C., and Y.X. conducted research; I.V., L.A.H., and D.C. provided essential reagents; D.C.R., M.S.L., and N.O.D. wrote the paper; and D.C.R. had primary responsibility for the final content. All authors read and approved the final manuscript.

Literature Cited

1. Levin MS, Rubin DC. Intestinal adaptation: the biology of the intestinal response to resection and disease. In: Langnas AN, Quigley EM, Tappenden KA, editors. Intestinal failure: diagnosis, management and transplantation. Malden (MA): Blackwell Publishing; 2008. p. xxi, 390.
2. Tappenden KA. Mechanisms of enteral nutrient-enhanced intestinal adaptation. Gastroenterology. 2006;130:S93–9.
3. Jeppesen PB. The use of hormonal growth factors in the treatment of patients with short-bowel syndrome. Drugs. 2006;66:581–9.
4. Gottschalck IB, Jeppesen PB, Hartmann B, Holst JJ, Henriksen DB. Effects of treatment with glucagon-like peptide-2 on bone resorption in colectomized patients with distal ileostomy or jejunostomy and short-bowel syndrome. Scand J Gastroenterol. 2008;43:1304–10.
5. Rubin DC, Swietlicki EA, Wang JL, Levin MS. Regulation of PC4/TIS7 expression in adapting remnant intestine after resection. Am J Physiol. 1998;275:G506–13.
6. Swietlicki E, Iordanov H, Fritsch C, Yi L, Levin MS, Rubin DC. Growth factor regulation of PC4/TIS7, an immediate early gene expressed during gut adaptation after resection. JPEN J Parenter Enteral Nutr. 2003;27:123–31.
7. Wang Y, Iordanov H, Swietlicki EA, Wang L, Fritsch C, Coleman T, Semenkovich CF, Levin MS, Rubin DC. Targeted intestinal overexpression of the immediate early gene tis7 in transgenic mice increases triglyceride absorption and adiposity. J Biol Chem. 2005;280:34764–75.
8. Vadivelu SK, Kurzbauer R, Dieplinger B, Zweyer M, Schafer R, Wernig A, Vietor I, Huber LA. Muscle regeneration and myogenic differentiation defects in mice lacking TIS7. Mol Cell Biol. 2004;24:3514–25.
9. Buhman KK, Wang LC, Tang Y, Swietlicki EA, Kennedy S, Xie Y, Liu ZY, Burkly LC, Levin MS, et al. Inhibition of Hedgehog signaling protects adult mice from diet-induced weight gain. J Nutr. 2004;134:2979–84.
10. Shaker A, Swietlicki EA, Wang L, Jiang S, Onal B, Bala S, Deschryver K, Newberry R, Levin MS, et al. Epimorphin deletion protects mice from inflammation-induced colon carcinogenesis and alters stem cell niche myofibroblast secretion. J Clin Invest. 2010;120:2081–93.
11. Schwarz M, Lund EG, Setchell KD, Kayden HJ, Zerwekh JE, Bjorkhem I, Herz J, Russell DW. Disruption of cholesterol 7alpha-hydroxylase gene in mice. II. Bile acid deficiency is overcome by induction of oxysterol 7alpha-hydroxylase. J Biol Chem. 1996;271:18024–31.
12. Bernal-Mizrachi C, Weng S, Li B, Nolte LA, Feng C, Coleman T, Holloszy JO, Semenkovich CF. Respiratory uncoupling lowers blood pressure through a leptin-dependent mechanism in genetically obese mice. Arterioscler Thromb Vasc Biol. 2002;22:961–8.
13. Li B, Nolte LA, Ju JS, Han DH, Coleman T, Holloszy JO, Semenkovich CF. Skeletal muscle respiratory uncoupling prevents diet-induced obesity and insulin resistance in mice. Nat Med. 2000;6:1115–20.
14. Chakravarthy MV, Zhu Y, Lopez M, Yin L, Wozniak DF, Coleman T, Hu Z, Wolfgang M, Vidal-Puig A, et al. Brain fatty acid synthase activates PPARalpha to maintain energy homeostasis. J Clin Invest. 2007;117:2539–52.
15. Carr TP, Andresen CJ, Rudel LL. Enzymatic determination of triglyceride, free cholesterol, and total cholesterol in tissue lipid extracts. Clin Biochem. 1993;26:39–42.
16. National Center for Biotechnology Information. Entrez Gene [cited 2010 Aug 3]. Available from: http://www.ncbi.nlm.nih.gov/sites/entrez?db=gene.
17. Tang Y, Swietlicki EA, Jiang S, Buhman KK, Davidson NO, Burkly LC, Levin MS, Rubin DC. Increased apoptosis and accelerated epithelial migration following inhibition of hedgehog signaling in adaptive small bowel postresection. Am J Physiol Gastrointest Liver Physiol. 2006;290:G1280–8.
18. Gilham D, Labonte ED, Rojas JC, Jandacek RJ, Howles PN, Hui DY. Carboxyl ester lipase deficiency exacerbates dietary lipid absorption abnormalities and resistance to diet-induced obesity in pancreatic triglyceride lipase knockout mice. J Biol Chem. 2007;282:24642–9.
19. Newberry EP, Xie Y, Kennedy SM, Luo J, Davidson NO. Protection against Western diet-induced obesity and hepatic steatosis in liver fatty acid-binding protein knockout mice. Hepatology. 2006;44:1191–205.
20. Tang Y, Swartz-Basile DA, Swietlicki EA, Yi L, Rubin DC, Levin MS. Bax is required for resection-induced changes in apoptosis, proliferation, and members of the extrinsic cell death pathways. Gastroenterology. 2004;126:220–30.
21. Vietor I, Huber LA. Role of TIS7 family of transcriptional regulators in differentiation and regeneration. Differentiation. 2007;75:891–7.
22. Vietor I, Vadivelu SK, Wick N, Hoffman R, Cotten M, Seiser C, Fialka I, Wunderlich W, Haase A, et al. TIS7 interacts with the mammalian SIN3 histone deacetylase complex in epithelial cells. EMBO J. 2002;21:4621–31.
23. Micheli L, Leonardi L, Conti F, Buanne P, Canu N, Caruso M, Tirone F. PC4 coactivates MyoD by relieving the histone deacetylase 4-mediated inhibition of myocyte enhancer factor 2C. Mol Cell Biol. 2005;25:2242–59.
24. Narisawa S, Huang L, Iwasaki A, Hasegawa H, Alpers DH, Millan JL. Accelerated fat absorption in intestinal alkaline phosphatase knockout mice. Mol Cell Biol. 2003;23:7525–30.
25. Wang ZQ, Watanabe Y, Noda T, Yoshida A, Oyama T, Toki A. Morphologic evaluation of regenerated small bowel by small intestinal submucosa. J Pediatr Surg. 2005;40:1898–902.
26. Hajri T, Hall AM, Jensen DR, Pietka TA, Drover VA, Tao H, Eckel R, Abumrad NA. CD36-facilitated fatty acid uptake inhibits leptin production and signaling in adipose tissue. Diabetes. 2007;56:1872–80.
27. Nauli AM, Nassir F, Zheng S, Yang Q, Lo CM, Vonlehmden SB, Lee D, Jandacek RJ, Abumrad NA, et al. CD36 is important for chylomicron formation and secretion and may mediate cholesterol uptake in the proximal intestine. Gastroenterology. 2006;131:1197–207.
28. Buhman KK, Smith SJ, Stone SJ, Repa JJ, Wong JS, Knapp FF Jr, Burri BJ, Hamilton RL, Abumrad NA, et al. DGAT1 is not essential for intestinal triacylglycerol absorption or chylomicron synthesis. J Biol Chem. 2002;277:25474–9.
29. Smith SJ, Cases S, Jensen DR, Chen HC, Sande E, Tow B, Sanan DA, Raber J, Eckel RH, et al. Obesity resistance and multiple mechanisms of triglyceride synthesis in mice lacking Dgat. Nat Genet. 2000;25:87–90.
30. Gu Y, Harley IT, Henderson LB, Aronow BJ, Vietor I, Huber LA, Harley JB, Kilpatrick JR, Langefeld CD, et al. Identification of IFRD1 as a modifier gene for cystic fibrosis lung disease. Nature. 2009;458:1039–42.
31. Vietor I, Kurzbauer R, Brosch G, Huber LA. TIS7 regulation of the beta-catenin/Tcf-4 target gene osteopontin (OPN) is histone deacetylase-dependent. J Biol Chem. 2005;280:39795–801.
32. Dieplinger B, Schiefermeier N, Juchum-Pasquazzo M, Gstir R, Huber LA, Klimaschewski L, Vietor I. The transcriptional corepressor TPA-inducible sequence 7 regulates adult axon growth through cellular retinoic acid binding protein II expression. Eur J Neurosci. 2007;26:3358–67.

33. Dekaney CM, Fong JJ, Rigby RJ, Lund PK, Henning SJ, Helmrath MA. Expansion of intestinal stem cells associated with long-term adaptation following ileocecal resection in mice. Am J Physiol Gastrointest Liver Physiol. 2007;293:G1013–22.
34. de Lau W, Barker N, Clevers H. WNT signaling in the normal intestine and colorectal cancer. Front Biosci. 2007;12:471–91.
35. Watt FM. Unexpected Hedgehog-Wnt interactions in epithelial differentiation. Trends Mol Med. 2004;10:577–80.
36. Xie Y, Luo J, Kennedy S, Davidson NO. Conditional intestinal lipotoxicity in Apobec-1−/− Mttp-IKO mice: a survival advantage for mammalian intestinal apolipoprotein B mRNA editing. J Biol Chem. 2007;282:33043–51.
37. Wang LC, Nassir F, Liu ZY, Ling L, Kuo F, Crowell T, Olson D, Davidson NO, Burkly LC. Disruption of hedgehog signaling reveals a novel role in intestinal morphogenesis and intestinal-specific lipid metabolism in mice. Gastroenterology. 2002;122:469–82.